Retracted: Formation Control of Multiple Mobile Robots Systems

Zhanfeng Li, Youliang Ma, and Tong Ren

Southwest University of Science and Technology, 621010 Mianyang, China
qlizhanfeng@163.com, mayouliang@swust.edu.cn, rentong64@163.com

Abstract. This paper presents a vision-based framework for mobile robot detection and tracking using off-the-shelf cameras mounted on mobile robots. Target detection and pose estimation are performed from single frames using fiducial markers as key elements. The method consists in distributing an octagon shaped structure on the back part of each robot. These shapes are easy to extract from the images and posses unique ID codes to facilitate pose estimation. Pose estimation algorithms method about Projection ray attraction (PRA) is programmed and compared. Finally, a dual Unscented Kalman filter (DUKF) is implemented to smooth measured data and estimate unknown leader's velocities.

Keywords: Pose estimation, Robot, Formation control.

1 System Overview

The visual tracking problem is divided in target detection and pose estimation. Target detection is related to image processing, whereas pose estimation is related to vision and nonlinear filtering.

The detection process is the most time consuming, but it can be simplified by using fiducial markers. In our vision system, Vision for mobile robot vision, markers are distributed on the back part of each robot on a truncated octagon shaped structure, as can be seen in Figure 1. Each face of this shape has a code that not only identifies the face, but also its position on the robot, as it is explained in the next Section. The ink patter is black and white to reduce lighting and camera sensitivity requirements.

Synthetic cameras are used for tuning and testing purposes, see Figure 2, and real cameras are used with a PC104 for the on-board image capture and processing system. Currently, Firewire IEEE-1394 and USB 2.0 cameras are supported, in particular, Unibrain's Fire-I, Point Grey's Bumblebee, and Logitech 3000 cameras.

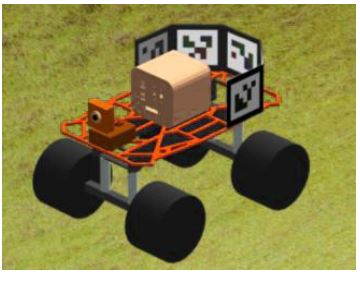

Fig. 1. Scheme of the TXT platform

C. Xiong et al. (Eds.): ICIRA 2008, Part I, LNAI 5314, pp. 75–82, 2008.

Fig. 2. Synthetic camera screen shot

Vision processing can be divided in the tasks resumed in the Figure 3.

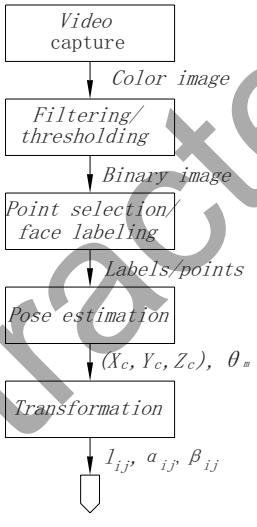

Fig. 3. Vision processing flow chart

2 Pose Estimation

Pose estimation refers to the issue of obtaining relative position and orientation between two or more mobile robots using a camera. This Section reviews the camera models and resumes the key points of the pose estimation methods used in this work.

2.1 Camera Model

The cameras used in this work are modeled with the well-know pinhole camera model.This model can be viewed as a box with a hole, or aperture, on one of its sides. This aperture allows light to enter into the box and reflect on the opposite side of the box, where light intensity can be measured, Figure 4 shows an schematic representation.

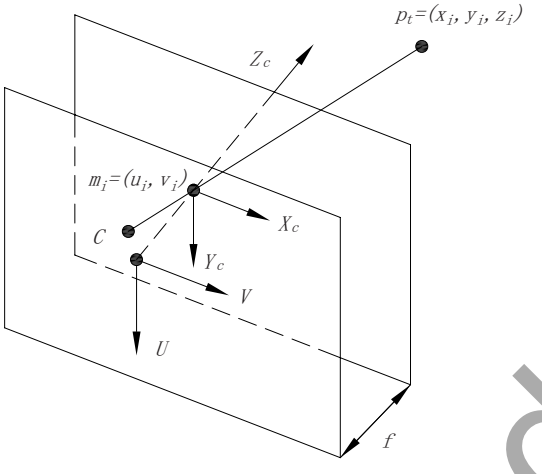

Fig. 4. Pinhole camera model

The projection of point pi on the image is given by:

$$m_i = \frac{1}{c_{z_i}} M p_i \tag{1}$$

where $M = K[R, t]$ and K denotes the intrinsic matrix transformation given by:

$$k = \begin{bmatrix} \alpha & \alpha \cot \theta_s & u_o \\ 0 & -\dfrac{\beta}{\sin \theta_s} & v_o \\ 0 & 0 & 1 \end{bmatrix} \tag{2}$$

2.2 OpenGL Camera Model

The main advantage of using a synthetic camera is the possibility of having its internal parameters perfectly known. OpenGL performs several transformations before drawing a point on the screen. This Section describes these transformations and obtains a synthetic intrinsic matrix transformation K_{OGL}.

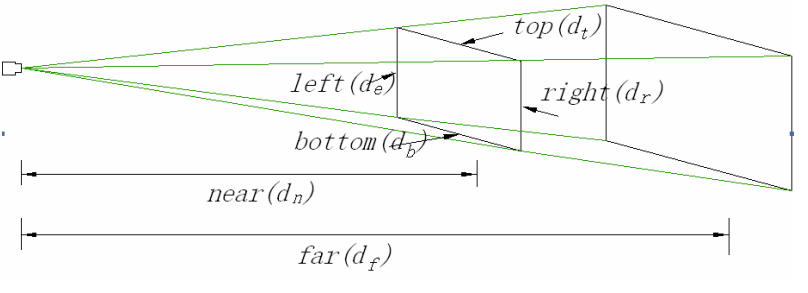

Fig. 5. OpenGL camera frustum

In Figure 5 OpenGL intrinsic matrix transformation K_{OGL} is given by.

$$\kappa_{OGL} = \begin{bmatrix} \frac{d_n w}{d_r - d_e} & 0 & \frac{d_e w}{d_r - d_e} & 0 \\ 0 & \frac{d_n h}{d_t - d_b} & \frac{d_b h}{d_t - d_b} & 0 \\ 0 & 0 & -\frac{d_f}{d_f - d_n} & -\frac{d_f d_n}{d_f - d_n} \end{bmatrix} \tag{3}$$

Therefore, by simple comparison, we can obtain the intrinsic parameters.

$$\theta = \frac{\pi}{2}, \alpha = \frac{d_n w}{d_r - d_e}, \beta = -\frac{d_n h}{d_t - d_b}, \mu_0 = \frac{d_e w}{d_r - d_e}, v_0 = \frac{d_b h}{d_t - d_b} \tag{4}$$

2.3 Pose Estimation Algorithms

Projection ray attraction (PRA) is a method presented to recover motion information from two-dimensional projections of a given three-dimensional point set.It is divided in two linear estimation parts: depth approximation and pose computation.In the depth approximation part, feature points in the three-dimensional space are estimated. In the pose computation part, rotation and translation parameters of the object are estimated using singular value decomposition (SVD). Both part are iteratively executed until the result is stable.

The main idea is to state pose estimation as a nonlinear optimization problem using a simplified camera model: Given a set of image points m_i, $i = 1, \ldots, N$, and three-dimensional feature points p_i, referred to the object coordinate frame, or ${}^c p_i$ referred to the camera coordinate frame, the pose estimation problem can be solved by minimizing the functional.

$$\min_{R,t,d_i} F(R,t,d_i) = \sum_{i=1}^{N} \| d_i v_i - (Rp_i + t) \|^2, \tag{5}$$

The minimization problem (6) is solved by SVD. Let H be defined as:

$$H = \frac{1}{N} \sum \| (M_i - \mu_M)({}^c p_i - \mu_p)^T \| \tag{6}$$

3 Nonlinear Filtering

In this Section, we resume the leader-follower an estimation algorithm using a dual unscented Kalman filter. The filter is used to smooth measured variables and to recover leader's velocities.

3.1 Nonlinear Observability

The observability codistribution *do(x)* is given by:

$$do(x) = span\{o_1, o_2, o_3, o_4, o_5, o_6, o_7\}, \tag{7}$$

With

$$
\begin{aligned}
O_1 &= [0,0,0,1,0,0] \\
O_2 &= [0,0,0,0,\sin\alpha_{12},0] \\
O_3 &= [0,0,0,0,\sin(\alpha_{12}+\theta_{12}),\sin(\alpha_{12}+\theta_{12})] \\
O_4 &= [0,0,0,0,1,0] \\
O_5 &= [0,0,0,\frac{\sin\alpha_{12}}{e_{12}^2},\frac{\cos\alpha_{12}}{e_{12}},0] \\
O_6 &= [0,0,0,\frac{\cos(\alpha_{12}+\theta_{12})}{e_{12}^2},\frac{\sin(\alpha_{12}+\theta_{12})}{e_{12}},\frac{\sin(\alpha_{12}+\theta_{12})}{e_{12}}] \\
O_7 &= [0,0,0,0,0,1]
\end{aligned}
\tag{8}
$$

It is clear that x_1, y_1, and θ_1 are unobservable.

3.2 The Dual Unscented Kalman Filter (DUKF)

The unscented Kalman filter (UKF) uses a deterministic sampling approach, the unscented transform (UT), to capture the mean and covariance estimates with a minimal set of sample points. When the sampling points are propagated through the true nonlinear system, the UKF can capture the posterior mean and covariance accurately up to the 3rd order for Taylor series expansion of the Gaussian error distribution with same order of computational complexity as the EKF that can achieve only up to first-order accuracy. It should also be noted that the of the UKF is the same order as that of EKF .

The state estimation filter considers the parameter known for state updating, whereas its parameter estimation counterpart considers states known for parameter updating.

In the leader-follower model the states are given by the vector X_k and the parameter by vector W_k. That is, leader's velocities are considered known for state estimation and then updated by the parameter estimation filter, as it is schematically represented in Figure 6. Note that there is no convergence guarantee with the DUKF.

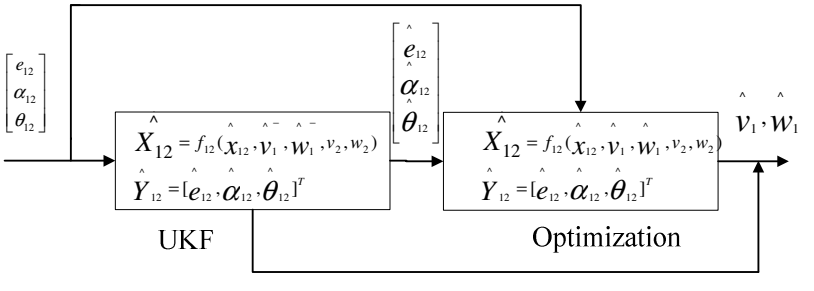

Fig. 6. Dual estimation problem

4 Simulation Results

Figures 7-8 show identification results for three robots. Figure 7 shows faces detected when the robots are in configurations q_1 = [1.5, .25, 0.0]^T and q_2 =[2.0,–0.45, 0.0]^T

Fig. 7. Identifications: Robot 1 (left) IDs 2, 3, 4, 5; robot 2 (ri[illegible]) IDs 1

Fig. 8. Identifications: Robot 1 (right) IDs 2, 3, 4; robot 2 (left) IDs 2, 3, 4

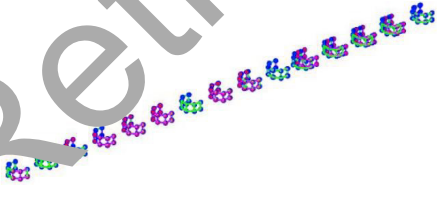

Fig. 9. Pure translation using Lowe's method

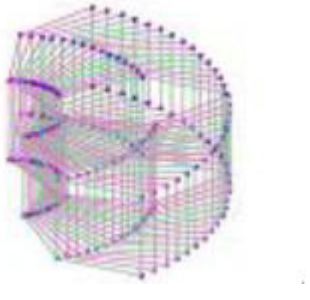

Fig. 10. Pure rotation using Lowe's method

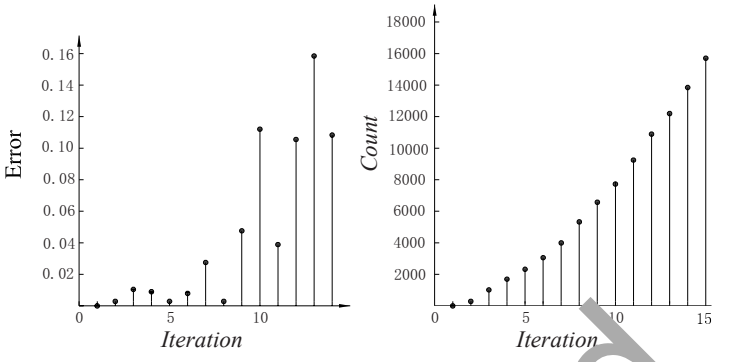

Fig. 11. Pure translation. Error and number of iterations using PRA method.

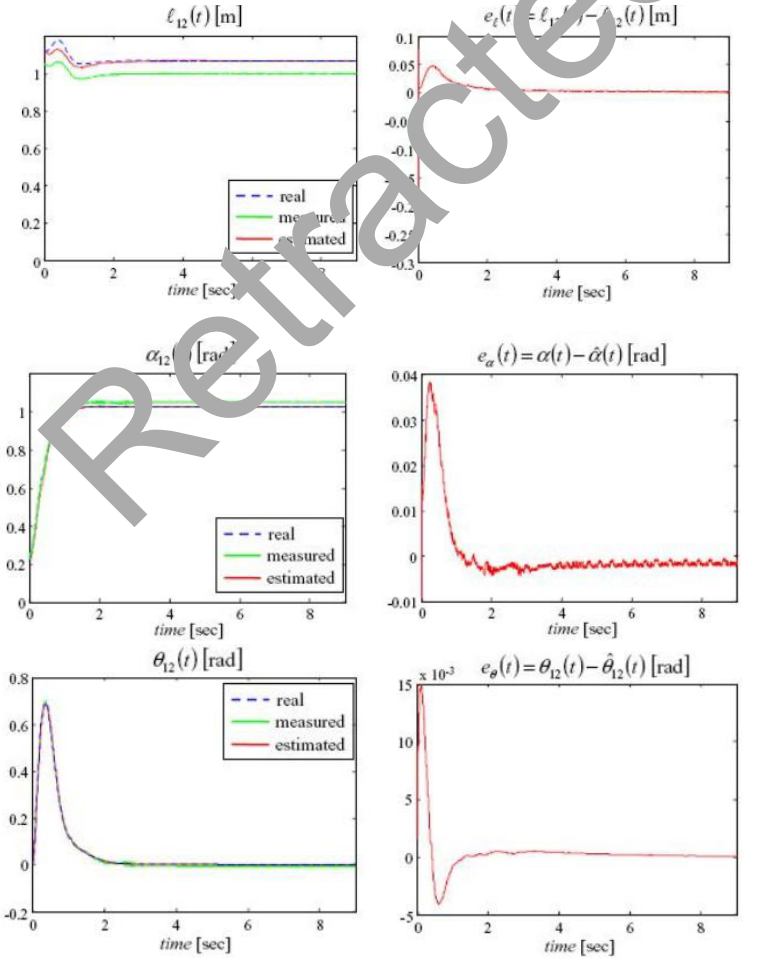

Fig. 12. Relative distance and bearing estimation using a DUKF

relative to the follower configuration. Figure 8 show same results with q_1 = [2.5,−0.5, 0.0]^T , q_2 = [3.5, 0.5, 0.0]^T , respectively. The algorithm performs very well, even with small surfaces, changes in illumination and increasing distance.

Figures 9 and 10 show estimated pose for pure translation and pure rotationmotions using Lowe's algorithm.

Figure 11 shows the error and number of iteration of PRA algorithm without using information from previous iterations. Figures 12 show estimation results with the DUKF in open loop.

5 Summary

This Chapter presents an architecture for model-based pose estimation for pairs of robots in formation. This architecture combines fiducial-based robot following, an pose estimation algorithms, and nonlinear filtering.

PRA algorithm requires notoriously more iterations to achieve convergence.

Fiducial marker detection performs very well in the simulations in a realistic 3D environment for distances between *30* cm and 2 m, and angles between $-\pi/2$ to$\pi/2$. Pose estimation algorithms give accurate measurements of relative distance and bearing.Finally, the implemented dual unscented Kalman filter notoriously improves measurements and is able to estimate unknown velocities. The main drawback of the current implementation is on feature detection. The method is sensitive to noise and change in lighting, but very fast to compute. Future research will focus results from the dual unscented Kalman filter with feature point extraction to increase robustness of the whole framework.

References

1. Or, S.H., Luk, W.S., Wong, K.H., King, I.: An eficient iterative pose estimation algorithm. Image and Vision Computing, 353–362 (1998)
2. Orqueda, O.A.A.: Motion Planning and Control of Autonomous Robots. Doctoral thesis, Universidad Nacional del Sur, Department of Electrical and Computer Engineering, Bahía Blanca, Argentina, pp. 35–43 (2006)
3. Shreiner, D., Woo, M., Neider, J., Davis, T.: OpenGL programming guide: The oficial guide to learning OpenGL, pp. 23–42. Addison-Wesley Professional, Reading (2005)
4. Wan, E.A., Van Der Merwe, R.: The Unscented Kalman Filter, pp. 52–112. Wiley Publishing, Chichester (2001)